JCI insight

Tubular β-catenin and FoxO3 interactions protect in chronic kidney disease

Stellor Nlandu-Khodo, … , Ethan Lee, Leslie S. Gewin

JCI Insight. 2020;5(10):e135454. https://doi.org/10.1172/jci.insight.135454.

Research Article | Cell biology | Nephrology

Graphical abstract

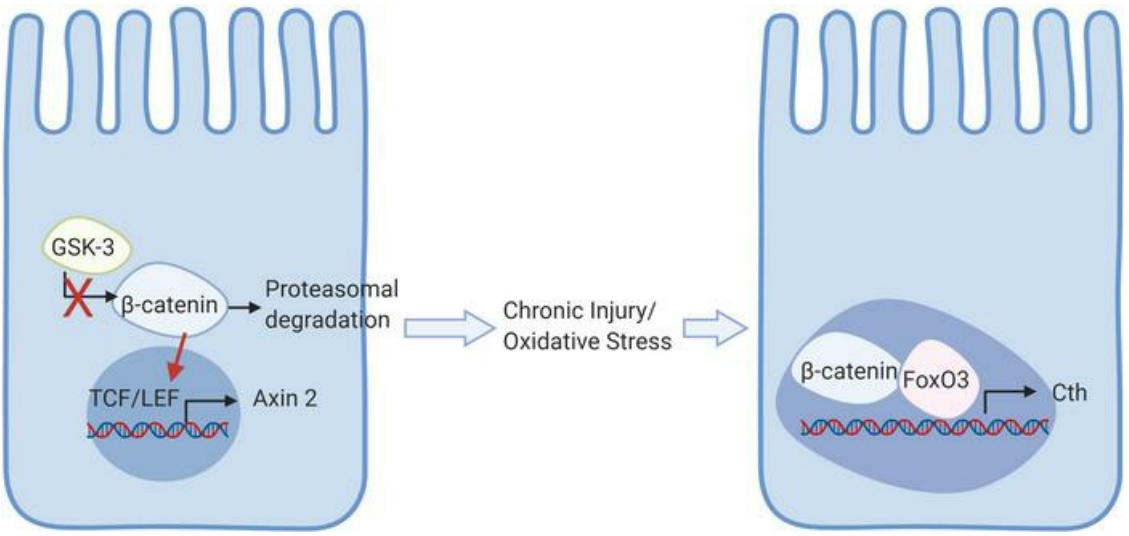

JCI insight

RESEARCH ARTICLE

Tubular β-catenin and FoxO3 interactions protect in chronic kidney disease

Stellor Nlandu-Khodo,[1,2] Yosuke Osaki,[1] Lauren Scarfe,[1] Haichun Yang,[3] Melanie Phillips-Mignemi,[1] Jane Tonello,[1] Kenyi Saito-Diaz,[4] Surekha Neelisetty,[1] Alla Ivanova,[1] Tessa Huffstater,[5] Robert McMahon,[1] M. Mark Taketo,[6] Mark deCaestecker,[1] Balakuntalam Kasinath,[7] Raymond C. Harris,[1,8,9] Ethan Lee,[4] and Leslie S. Gewin[1,4,9]

[1]Division of Nephrology and Hypertension, Department of Medicine, Vanderbilt University Medical Center (VUMC), Nashville, Tennessee, USA. [2]Institute of Physiology, University of Zurich, Zurich, Switzerland. [3]Department of Pathology, Microbiology and Immunology, VUMC, Nashville, Tennessee, USA. [4]Department of Cell and Developmental Biology and [5]Department of Biomedical Engineering, Vanderbilt University, Nashville, Tennessee, USA. [6]Division of Experimental Therapeutics, Graduate School of Medicine, Kyoto University, Kyoto, Japan. [7]Department of Medicine, Long School of Medicine, University of Texas Health San Antonio, San Antonio, Texas, USA. [8]Department of Molecular Physiology and Biophysics, Vanderbilt University, Nashville, Tennessee, USA. [9]Department of Medicine, Veterans Affairs Hospital, Tennessee Valley Healthcare System, Nashville, Tennessee, USA.

The Wnt/β-catenin signaling pathway plays an important role in renal development and is reexpressed in the injured kidney and other organs. β-Catenin signaling is protective in acute kidney injury (AKI) through actions on the proximal tubule, but the current dogma is that Wnt/β-catenin signaling promotes fibrosis and development of chronic kidney disease (CKD). As the role of proximal tubular β-catenin signaling in CKD remains unclear, we genetically stabilized (i.e., activated) β-catenin specifically in murine proximal tubules. Mice with increased tubular β-catenin signaling were protected in 2 murine models of AKI to CKD progression. Oxidative stress, a common feature of CKD, reduced the conventional T cell factor/lymphoid enhancer factor–dependent β-catenin signaling and augmented FoxO3-dependent activity in proximal tubule cells in vitro and in vivo. The protective effect of proximal tubular β-catenin in renal injury required the presence of FoxO3 in vivo. Furthermore, we identified cystathionine γ-lyase as a potentially novel transcriptional target of β-catenin/FoxO3 interactions in the proximal tubule. Thus, our studies overturned the conventional dogma about β-catenin signaling and CKD by showing a protective effect of proximal tubule β-catenin in CKD and identified a potentially new transcriptional target of β-catenin/FoxO3 signaling that has therapeutic potential for CKD.

Introduction

Chronic kidney disease (CKD) affects nearly 15% of the American population (1) with a global prevalence of more than 11% (2) and presents a high economic burden as well as increased cardiovascular morbidity and mortality. Acute kidney injury (AKI), commonly caused by sepsis, drugs, and ischemia, often appears to resolve by measures of renal function but independently increases the risk of CKD development and progression (3). AKI conversion to CKD is a complex process involving many cell types, but the proximal tubule is arguably the central player because it is the target of acute injury. Others have shown that isolated injury to the proximal tubule, if severe enough or repetitive, is sufficient to cause tubular atrophy and renal fibrosis, the hallmark of CKD (4, 5). In response to injury, the proximal tubule undergoes changes in cell cycle, differentiation, and metabolism, and these proximal tubule–specific responses may determine whether the kidney undergoes successful repair or progresses to CKD after injury.

The injured proximal tubule recapitulates expression of many growth factors that are involved in renal development. The Wnt/β-catenin pathway is critical for renal development but quiescent in the uninjured adult kidney with the exception of the renal medulla (6–8). β-Catenin has dual roles, functioning as part of the adherens junction complex at the cell membrane but also acting as a transcription factor. In the absence of Wnt ligands, cytosolic β-catenin is normally targeted for degradation by glycogen synthase kinase-3 (GSK-3), a component of the destruction complex including Axin, adenomatous polyposis coli, and casein

Authorship note: SNK and YO contributed equally to this work.

Conflict of interest: The authors have declared that no conflict of interest exists.

Submitted: December 3, 2019
Accepted: April 22, 2020
Published: May 21, 2020.

Reference information: *JCI Insight*. 2020;5(10):e135454. https://doi.org/10.1172/jci.insight.135454.

kinase 1. When 1 of the 19 Wnt ligands binds to the frizzled receptor and the LDL-receptor-related protein 5/6 coreceptors, β-catenin escapes degradation and accumulates in the nucleus (9). Nuclear β-catenin, in complex with T cell factor/lymphoid enhancer factor (TCF/LEF), activates Wnt target genes to modulate cellular responses, such as proliferation, survival, and differentiation.

Wnt/β-catenin signaling increases after renal injury, particularly in the renal tubules (10–12). Several studies show that β-catenin activity is protective in AKI, primarily by either reducing apoptosis or enhancing proliferation in the proximal tubules (11, 13–15). By contrast, studies that overexpress Wnt ligands or block β-catenin signaling systemically suggest that this growth factor promotes fibrosis in CKD (16–19). In addition, activating Wnt/β-catenin in renal tubule cells in vitro causes dedifferentiation (20), and persistently dedifferentiated epithelial cells play an important role in the AKI-to-CKD transition (21). However, no studies to date have shown how augmenting β-catenin signaling exclusively in the proximal tubule, a key target of renal injury, affects CKD. To address this, we conditionally stabilized (i.e., activated) β-catenin in the proximal tubules after birth and used 2 models of AKI to CKD. Contrary to the conventional dogma that β-catenin promotes chronic injury and fibrosis, mice with increased β-catenin activity specifically in the proximal tubule were protected from kidney fibrosis and epithelial injury. This protection was dependent upon the expression of the transcription factor FoxO3, which can mediate stress responses such as antioxidant production, cell cycle arrest, and altered cell survival (22). Furthermore, we identified potentially novel downstream transcriptional targets of β-catenin and FoxO3 interactions that may inform new therapies for CKD.

Results

Increased β-catenin activity in proximal tubules is protective in AKI to CKD models. We generated mice with increased β-catenin activity in the proximal tubule by crossing *Ggt-Cre* mice (23) with *Ctnnb1*$^{ex3fl/fl}$ mice in which the phosphorylation site targeting β-catenin for degradation is floxed (24). Nuclear β-catenin protein expression (i.e., transcriptionally active β-catenin) from renal cortices was increased in the *Ggt-Cre Ctnnb1*$^{ex3fl/fl}$ mice, consistent with recombination (Supplemental Figure 1, A and B; supplemental material available online with this article; https://doi.org/10.1172/jci.insight.135454DS1). In addition, transcripts of *Axin2*, a well-characterized endogenous readout for β-catenin and TCF/LEF signaling (25), were increased 10-fold compared with floxed WT mice (Supplemental Figure 1C). Proximal tubule localization of β-catenin activity was confirmed by crossing the mice with Topflash reporter (*Tcf/Lef:H2B-GFP*) mice (26) and costaining with lotus tetragonolobus (LTL), a lectin specific for proximal tubules (Supplemental Figure 1D). No differences between the uninjured *Ggt-Cre Ctnnb1*$^{ex3fl/fl}$ and floxed WT mice were noted (Figure 1A). The mice were injured with aristolochic acid, a cause of acute to chronic kidney injury that targets the proximal tubule in humans and causes cell death acutely but later results in interstitial fibrosis (27, 28). Six weeks after AAN, tubular injury was significantly attenuated in the *Ggt-Cre Ctnnb1*$^{ex3fl/fl}$ mice, as measured by tubular injury scores (see Methods) and expression of KIM-1 (*Havcr1*), an indicator of proximal tubule injury, compared with floxed littermates (Figure 1, A–C). Tubulointerstitial fibrosis was also reduced in the mice with conditional β-catenin stabilization according to picrosirius red staining as well as collagen I transcripts (Figure 1, D–F), and renal function, measured by blood urea nitrogen (BUN), was better preserved (Figure 1G).

We then subjected our mice to another AKI to CKD model induced by unilateral ischemia/reperfusion injury (IRI) followed by contralateral nephrectomy 8 days later, and the mice were sacrificed 4 weeks after the ischemic event. Similar to the AAN model, the *Ggt-Cre Ctnnb1*$^{ex3fl/fl}$ mice had significantly reduced KIM-1 (*Havcr1*) and BUN compared with floxed littermates (Figure 1, H–J). To further characterize proximal tubule injury, we stained LTL, a lectin expressed on the brush border specifically of differentiated proximal tubules (29). There was significantly increased expression in the *Ggt-Cre Ctnnb1*$^{ex3fl/fl}$ compared with floxed controls after IRI, indicating less epithelial dedifferentiation after injury (Figure 1, K and L). There was a trend toward reduction in collagen transcripts in the *Ggt-Cre Ctnnb1*$^{ex3fl/fl}$ mice, but it did not reach statistical significance ($P = 0.06$, Figure 1M). Taken together, these data indicate that increasing β-catenin signaling in proximal tubules protects against tubule injury and preserves function in 2 models of AKI to CKD.

Augmenting β-catenin signaling protects against tubule epithelial apoptosis. Given the tubular protection in injured *Ggt-Cre Ctnnb1*$^{ex3fl/fl}$ mice, reflected by decreased KIM-1 levels and BUN after both AAN and IRI, we investigated how β-catenin signaling affected epithelial apoptosis. There were fewer TUNEL$^+$ cortical tubule cells, a measure of apoptosis/necrosis, in AAN-injured mice with β-catenin stabilized in proximal tubules compared with floxed controls (Figure 2, A and B). We used conditionally immortalized proximal tubule (PT) cells previously isolated and characterized (30) and exposed them to AA for 7 days in vitro to mimic

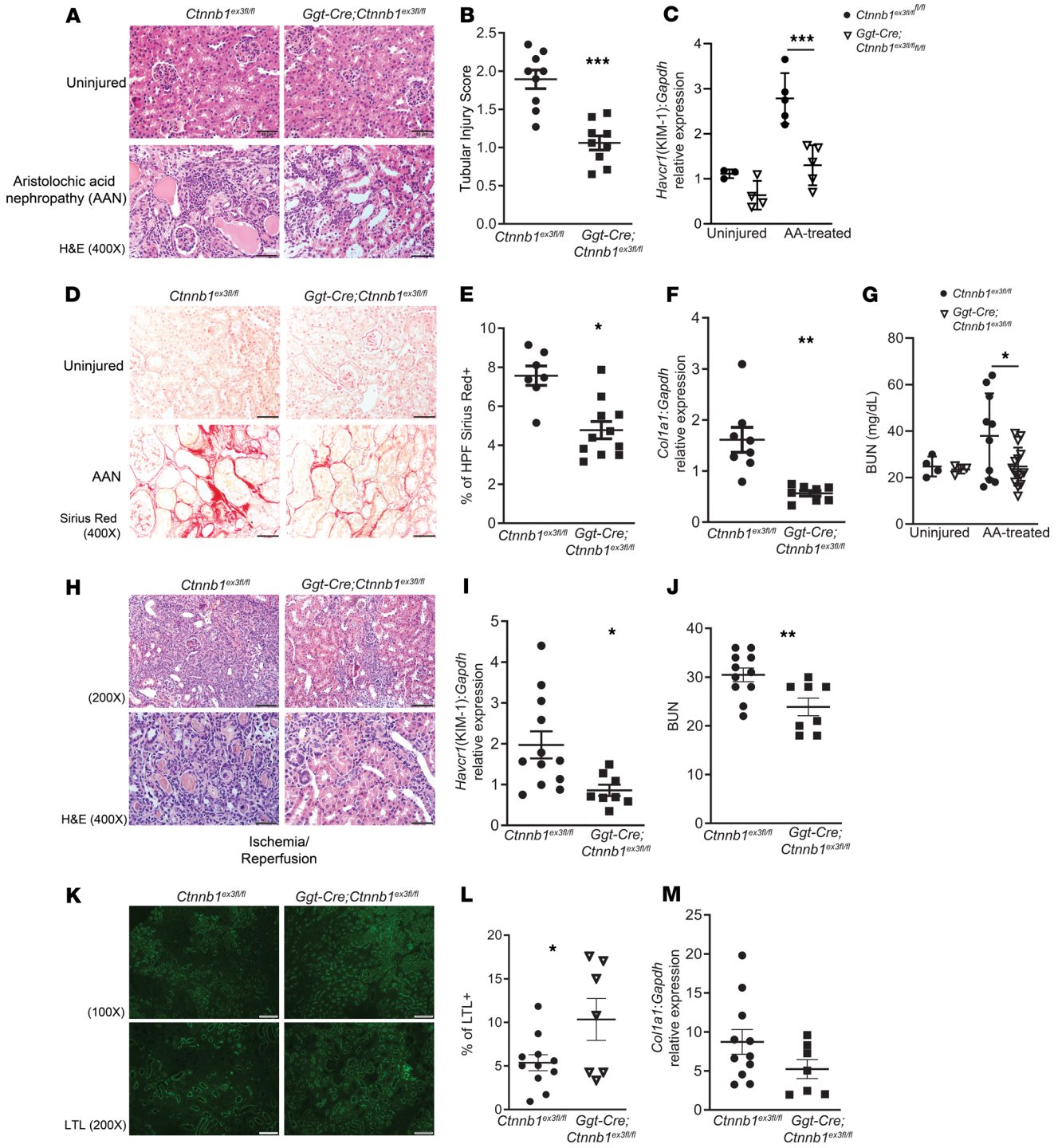

Figure 1. Increased β-catenin signaling in proximal tubules protects against AKI to CKD injury. (**A**) H&E sections of *Ggt-Cre Ctnnb1*$^{ex3fl/fl}$ mice and floxed controls without injury as well as 6 weeks after aristolochic acid nephropathy (AAN). Scale bars: 50 μm. (**B**) Injury was scored by colleagues who did not know the identity of the genotype (see Methods for scoring system). (**C**) KIM-1 (*Havcr1*) levels were measured by quantitative PCR, normalized to *Gapdh*, in cortical tissue from both uninjured and aristolochic acid–treated mice. (**D** and **E**) Picrosirius red (Sirius Red) staining measured collagen (red staining) and was quantified using ImageJ (NIH). Scale bar: 50 μm. (**F**) Collagen I (*Col1a1*) transcripts were measured by quantitative PCR (qPCR), normalized to *Gapdh*, from renal cortices 6 weeks after AAN. (**G**) Blood urea nitrogen (BUN) was measured from mice either uninjured or 6 weeks after AAN. (**H**) H&E from *Ggt-Cre Ctnnb1*$^{ex3fl/fl}$ mice and floxed controls injured by IRI and sacrificed 4 weeks later (see Methods for details). Scale bar: 100 μm for original magnification ×200 and 50 μm for ×400. (**I**) KIM-1 (*Havcr1*) expression in renal tissue after IRI injury and (**J**) BUN levels were measured at the time of sacrifice (4 weeks after IRI). (**K**) Staining for lotus tetragonolobus (LTL) conjugated to GFP was done. Scale bar: 100 μm for original magnification ×200 and 200 μm for ×100 (**K**) and quantified by ImageJ (**L**). (**M**) Collagen (*Col1a1*) levels were measured by qPCR from renal tissue 4 weeks after IRI. For all qPCR studies after IRI, the inner medulla was dissected away and discarded. Statistical analyses were done using the Student's *t* test with $*P < 0.05$, $**P < 0.01$, and $***P < 0.001$. For the AAN injury, 1 *Ctnnb1*$^{ex3fl/fl}$ mouse died before the study's completion, and for the IRI model, 1 mouse per genotype died prematurely.

chronic exposure. The AA-induced apoptosis, detected by cleaved caspase-3, was significantly reduced by treatment with a GSK-3 inhibitor (BIO), which augments β-catenin signaling (Figure 2, C and D). Because GSK-3 inhibitors can have β-catenin–independent effects, we also treated PT cells with the Wnt3a ligand, upregulated in renal injury (31), and saw a significant reduction in AA-induced apoptosis (Figure 2, E and F). Thus, increasing β-catenin signaling in PT cells reduced apoptosis in vivo and in vitro after AA exposure.

Oxidative stress alters β-catenin–dependent transcriptional activity. Others have reported that oxidative stress changes β-catenin's nuclear binding partners from TCF/LEF- to FoxO-dependent transcription, but this has not been investigated in tubular injury (32). The FoxO transcription factors play a critical role in regulating oxidative stress, proliferation, and cell survival, so this transcriptional switch may explain the protective effect of β-catenin in injured epithelia. In oxidative stress, FoxO1/3 transcription factors are thought to competitively inhibit TCF/LEF binding to β-catenin and, hence, TCF/LEF-dependent transcription (33, 34). As expected, Wnt3a ligand dose-dependently increased the expression of axin2, but the presence of oxidative stress (100 μM H_2O_2) greatly attenuated the Wnt3a-dependent axin2 expression (Figure 3A). To further investigate the effect of oxidative stress on β-catenin– and TCF/LEF-dependent activity, we stably transfected our PT cells with the Topflash reporter, a direct indicator of TCF/LEF-dependent β-catenin signaling (35). The addition of Wnt3a augmented the luminescent signal but was attenuated in the presence of oxidative stress (H_2O_2) (Figure 3B). These assays both show that oxidative stress reduces TCF/LEF-dependent β-catenin activity in PT cells.

We then asked whether the oxidative stress–dependent decrease in LEF/TCF-dependent β-catenin signaling was accompanied by increased FoxO activity. We showed that AA increases oxidative stress in PT cells in vitro with nitrotyrosine immunoblots (Figure 3C). The presence of AA and the Wnt3a ligand synergistically increased nuclear FoxO1 and FoxO3, with the latter being more abundant in PT cells (Figure 3, D and E). Nuclear FoxO1/3 is thought to represent active FoxO1/3, and the presence of both AA and Wnt3a was required to significantly raise FoxO activity. To determine whether oxidative stress induces FoxO3 nuclear binding to β-catenin, we performed coimmunoprecipitation studies of nuclear isolates with or without H_2O_2 (oxidative stress) and Wnt3a. Indeed, β-catenin and FoxO3 form a complex in the nucleus but only in the presence of both oxidative stress and Wnt3a (Figure 3, F and G). Furthermore, treatment with Wnt3a increased nuclear β-catenin as expected, and oxidative stress did not enhance nuclear β-catenin, suggesting that the increased binding of nuclear FoxO3 with β-catenin under oxidative stress was not due to increased nuclear β-catenin expression (Figure 3, F and H). In summary, oxidative stress reduces β-catenin–dependent LEF/TCF transcriptional responses while increasing FoxO3 activity and potentially transcriptional binding between β-catenin and FoxO3.

We then investigated how these oxidative stress–dependent alterations in TCF/LEF and FoxO3 activity affect the PT's response to AA-induced injury. We knocked down *Foxo3* using siRNA (Figure 4A) and showed that reduced FoxO3 potentiated apoptosis in PT cells treated with AA (Figure 4, B and C). To block β-catenin/TCF/LEF interactions, we used ICG-001, a small-molecule inhibitor of β-catenin/TCF signaling widely used to block these interactions (36). AA-induced apoptosis in PT cells was significantly reduced with the addition of ICG-001 (Figure 4, D and E). Taken together, these data suggest that switching β-catenin away from TCF/LEF-dependent and toward FoxO3-dependent signaling protects PT cells from AA-induced apoptosis.

Injured PTs with β-catenin stabilized have increased Foxo3 expression, which is necessary for a protective effect. We wanted to verify that this β-catenin–dependent increased FoxO3 activity in oxidative stress was present in vivo. AA induces oxidative stress, and the *Ggt-Cre Ctnnb1*$^{ex3fl/fl}$ mice had more LTL$^+$ tubules (i.e., PTs) with FoxO3 staining after AAN compared with floxed controls (Figure 5, A and B). However, consistent with the greater injury sustained and higher KIM-1 (*Havcr1*) expression, the floxed control mice had fewer LTL$^+$ tubules because this lectin is expressed on the brush border, which is lost in severe injury. Therefore, we also quantified the total number of FoxO3$^+$ cortical tubules, which was significantly higher in the *Ggt-Cre Ctnnb1*$^{ex3fl/fl}$ mice (Figure 5C). We confirmed that most FoxO3 staining was nuclear (i.e., active FoxO3) by merging FoxO3 with DAPI (Figure 5D).

We next investigated whether this augmented FoxO3 activity was required for the β-catenin–dependent protective effect in PT cells in vivo. We crossed the *Ggt-Cre Ctnnb1*$^{ex3fl/fl}$ with *Foxo3*$^{fl/fl}$ mice to generate double-transgenic mice with PT-specific increased β-catenin activity and deleted FoxO3 (*Ggt-Cre Ctnnb1*$^{ex3fl/fl}$ *Foxo3*$^{fl/fl}$). Recombination was verified by measuring Axin2 transcripts in renal cortices and FoxO3 from primary cortical tubule cells of injured mice (Supplemental Figure 2, A and B). After AAN, robust injury was induced in both the double conditional knockout and the floxed controls, but

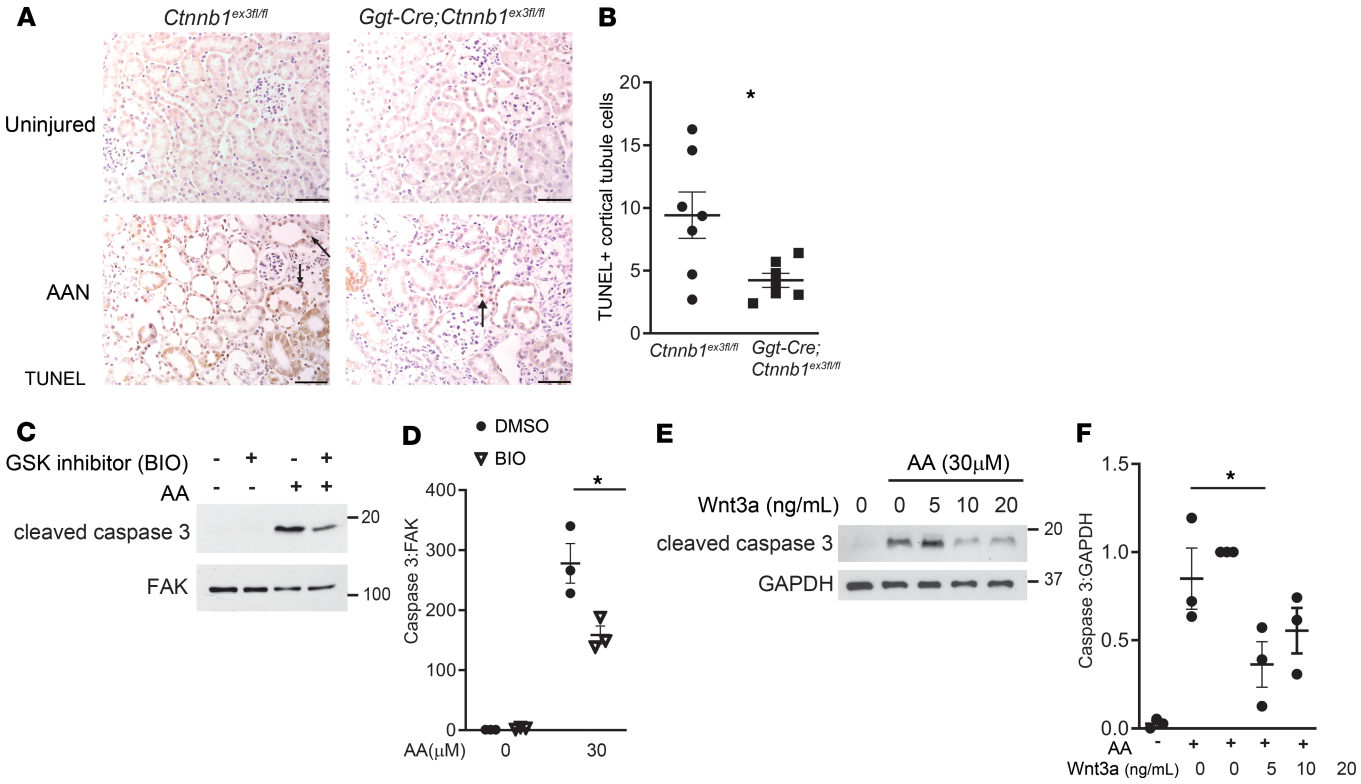

Figure 2. Increased β-catenin signaling protects against apoptosis in vivo and in vitro. (**A**) TUNEL staining was performed to detect apoptotic/necrotic cells in uninjured kidneys and those 6 weeks after aristolochic acid (AA) exposure. Scale bar: 50 μm. Arrows point to TUNEL$^+$ cortical tubule nuclei. (**B**) The TUNEL$^+$ cortical tubule cells were quantified by counting 10 views (at original magnification ×400) per kidney, and the fields were chosen and TUNEL$^+$ cells counted by personnel blinded to the genotype. (**C**) Proximal tubule (PT) cells in vitro were treated with AA 30 μM for 7 days with a GSK-3 inhibitor (BIO) added to some cells for the last 48 hours of treatment. (**D**) Cell lysates were immunoblotted for cleaved caspase-3, a measurement of apoptosis, and focal adhesion kinase (FAK) for loading control. (**E** and **F**) PT cells were also treated with AA ± Wnt3a ligand with a statistically significant decrease in AA-induced apoptosis with 10 ng/mL of Wnt. Student's *t* test was used for statistical comparisons between 2 groups in **B** and **D**, and ANOVA for multiple comparisons was used for **F** with $^*P < 0.05$. For each of the 3 experiments in **E** and **F**, the value of Wnt3a at 5 ng/mL was normalized to 1 and others expressed relative to this with each value compared with AA without Wnt3a (control).

the BUN and KIM-1 levels were not significantly different at 6 weeks after injury between the 2 genotypes (Figure 5, E–G). Furthermore, measurements of fibrosis (collagen I transcripts by qPCR and picrosirius red staining) showed a nonsignificant trend toward the double–conditional knockout mouse having more rather than less fibrosis (Figure 5, H–J). In summary, the protective effect noted previously in mice with PT-specific β-catenin stabilization requires the presence of FoxO3.

Cystathionine γ-lyase is a potentially novel target of β-catenin/FoxO3. Most of β-catenin's downstream effects have been described in the context of β-catenin's interactions with TCF/LEF without regard for oxidative stress's impact on β-catenin's downstream transcriptional targets. The β-catenin/FoxO complex was shown to be protective in inflammatory cells in the context of TGF-β–induced injury (36), but the downstream targets mediating this protective effect were not identified. We used RNA-Seq to identify novel targets of β-catenin/FoxO in renal epithelial cells that may be mediating this protective effect in injury. PT cells were treated with scramble, *Foxo1*, or *Foxo3* siRNA; β-catenin was activated with Wnt3a; and oxidative stress was induced with H_2O_2 (Figure 6A). There were no statistically significant differences in transcripts between scramble and *Foxo1* siRNA, but 12 genes were suppressed and 7 augmented by *Foxo3* siRNA (Table 1). Some of these FoxO3-regulated genes have been previously described as targets of β-catenin, such as *Ctgf* and *Serpine1* (37, 38). However, *Cth*, which codes for cystathionine γ-lyase (CSE), is, as far as we are aware, a novel target of β-catenin/FoxO3. CSE catalyzes the formation of hydrogen sulfide (H_2S) and the antioxidant glutathione, and renoprotective roles for both CSE and H_2S have been described (39–41).

We used qPCR to confirm reduction of *Cth* in *Foxo3* siRNA–treated PT cells treated with Wnt3a but only in the presence of H_2O_2-induced oxidative stress (Figure 6B). In addition, a GSK-3 inhibitor augmented CSE protein expression in AA-treated PT cells (Figure 6, C and D). Knockdown of *Cth* exacerbated

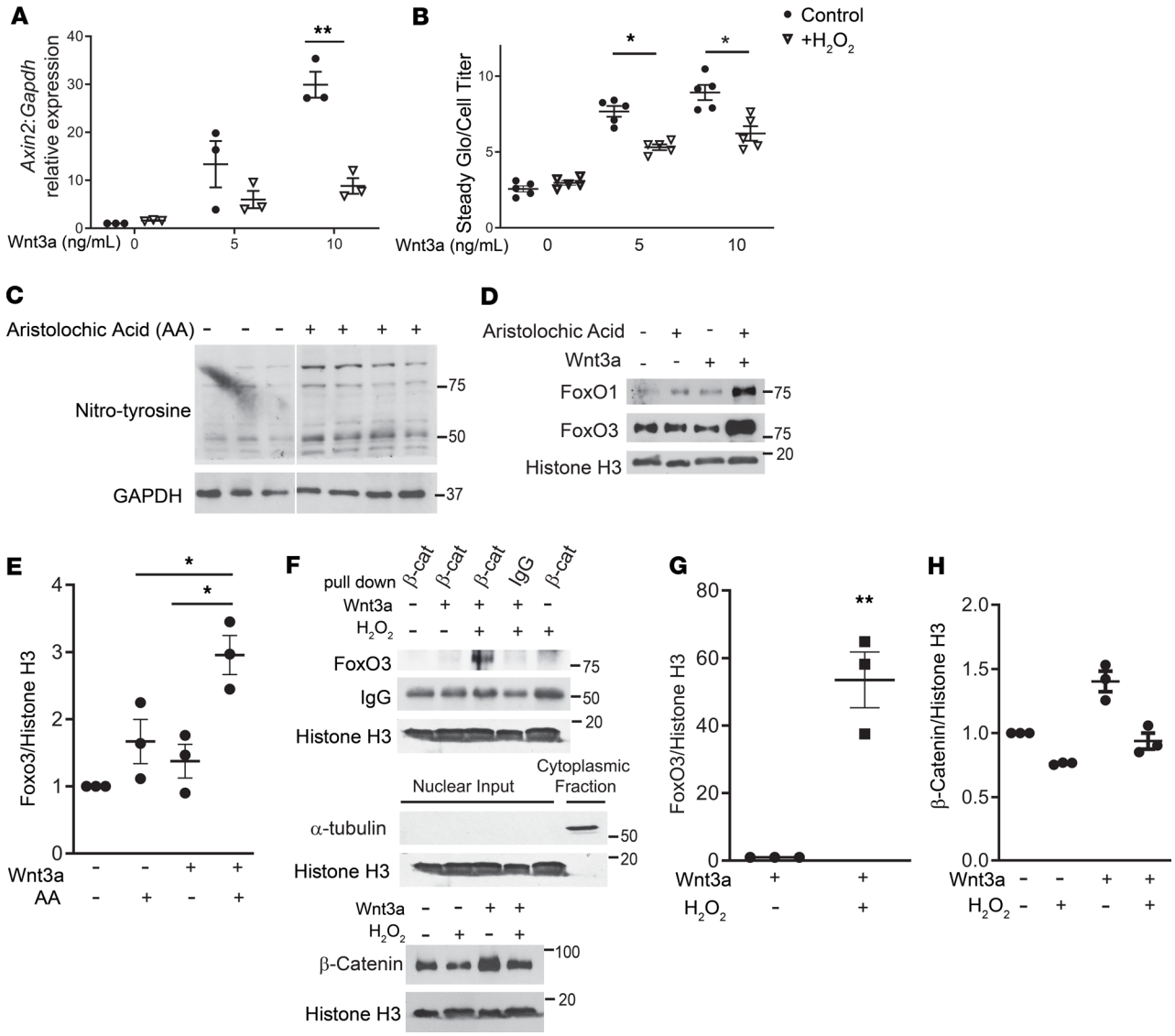

Figure 3. Oxidative stress reduces β-catenin/LEF/TCF-dependent signaling and augments β-catenin/FoxO signaling. (**A**) PT cells were treated with varying doses of Wnt3a either in control conditions (PT medium as described in Methods) or with oxidative stress (H_2O_2 100 μM in serum-free DMEM/F12) for 16 hours, and *Axin2* transcripts were measured by qPCR and normalized to *Gapdh*. (**B**) PT cells stably transfected with a Topflash reporter construct (see Methods) were treated with various doses of Wnt3a in either control or oxidative stress medium (H_2O_2 100 μM in serum-free DMEM/F12). A luminometer measured the TCF/LEF-dependent activity (Steady Glo), which was normalized to cell number by using Cell Titer assay. For both **A** and **B**, Holm-Šídák multiple-comparisons test was used. (**C**) Cells treated with AA for 5 days showed increased oxidative stress reflected by increased nitrotyrosine on immunoblots. PT cells were treated with AA (30 μM), Wnt3a (10 ng/mL) was added during the last 48 hours, and nuclei were isolated (see Methods) and immunoblotted for FoxO1, FoxO3, or histone H3 for loading (**D**), and the results from 3 separate experiments were quantified (**E**). (**F**) PT cells were treated ± Wnt3a (10 ng/mL) and oxidative stress (H_2O_2 100 μM) for 16 hours, and then nuclei were isolated and coimmunoprecipitation was performed. Nuclear isolates had either β-catenin pull-down or IgG control, then were immunoblotted with FoxO3, and histone H3 was used for loading control of nuclear input. The nuclear input was also immunoblotted with α-tubulin, to assess for nuclear purity, and β-catenin. Levels of FoxO3 from the coimmunoprecipitation, normalized to histone H3 (nuclear input), were quantified from 3 separate experiments (**G**), as were nuclear β-catenin levels (**H**). Student's *t* test was used for statistical analyses in **G** and **H**, and ANOVA was used for multiple comparisons in **E** with $*P < 0.05$ and $**P < 0.01$.

AA-induced apoptosis, suggesting that this target is a potential mediator of epithelial β-catenin/FoxO3-dependent cytoprotection (Figure 6, E and F). We then assessed whether CSE expression was altered in injured mice with β-catenin stabilized in the PT. CSE was markedly upregulated in cortical lysates of AAN-injured *Ggt-Cre Ctnnb1*$^{ex3fl/fl}$ mice compared with floxed controls (Figure 7, A and B). Staining for CSE revealed its distribution to be primarily in cortical tubules, consistent with PTs, in uninjured mice (Figure 7C). The levels of *Cth* transcripts also decreased in both genotypes after chronic injury, but levels in the AAN-injured *Ggt-Cre Ctnnb1*$^{ex3fl/fl}$ mice were significantly higher compared with those of the injured floxed

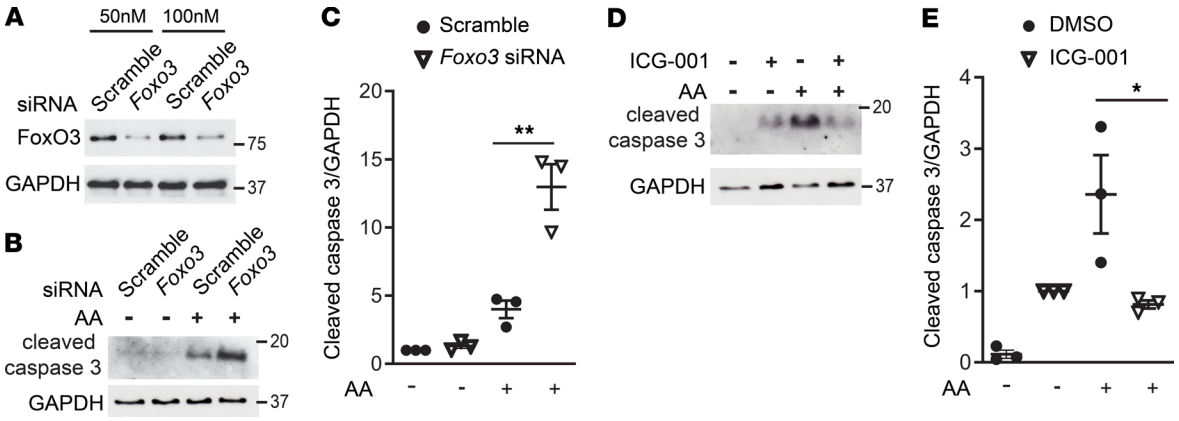

Figure 4. Inhibiting FoxO3 in PT cells increases while ICG-001 reduces AA-induced apoptosis. (**A**) We effectively reduced FoxO3 expression in PT cells by immunoblots using siRNA. (**B**) PT cells treated with *Foxo3* or scramble siRNA were treated with AA, and apoptosis was measured by cleaved caspase-3 on immunoblots with GAPDH as loading control. (**C**) The results of 3 independent studies were quantified by ImageJ. (**D**) PT cells were treated ± AA (30 μM for 7 days) and ICG-001 to inhibit β-catenin/TCF/LEF for the last 4 days and then lysates blotted for cleaved caspase-3 and GAPDH for loading. (**E**) Three experiments with AA + ICG-001 or DMSO (diluent control) are quantified, and the data were normalized to AA + DMSO. Student's *t* test was used for statistical comparisons with $^{*}P < 0.05$ and $^{**}P < 0.01$. GAPDH, glyceraldehyde 3, phosphate dehydrogenase.

littermates (Figure 7D). The augmented CSE expression noted in conditionally β-catenin–stabilized mice (Figure 7A) was erased when FoxO3 was also deleted (Figure 7E). In summary, CSE was identified as a novel target of β-catenin and FoxO3 in oxidative stress, knockdown of *Cth* worsened AA-induced apoptosis in vitro, and injured mice with increased tubular β-catenin activity had increased CSE protein expression and *Cth* transcripts compared with floxed controls.

Discussion

The PT plays a critical role in renal injury by either facilitating repair or mediating AKI progression to CKD, and growth factors play an important role in both processes. The role of β-catenin signaling in proximal tubular responses to chronic injury had not been well delineated. The current studies reveal a potentially novel protective pathway in the progression of AKI to CKD by showing (a) cell-autonomous β-catenin signaling in the PT protects against fibrosis and preserves renal function in 2 AKI to CKD models, (b) proximal tubular β-catenin activity enhances active (i.e., nuclear) FoxO3 in oxidative stress in vitro, (c) the protective effect of proximal tubular β-catenin in vivo requires the presence of FoxO3, and (d) CSE is a novel downstream target of β-catenin/FoxO3 in renal tubules and may mediate some of the antiapoptotic and antioxidant actions of these transcription factors.

Our finding that proximal tubular β-catenin protects against the development of CKD may be surprising given the many reports of β-catenin as a profibrotic factor in chronic injury. This paradigm of β-catenin as a mediator of fibrosis in CKD is largely based upon studies in which Wnt ligands are overexpressed or systemic inhibitors are used. Because Wnt ligands are soluble, even though they may be produced by tubules, they clearly have potent profibrotic actions on surrounding fibroblasts and pericytes (17, 42, 43). The other caveat about genetic overexpression of Wnts, or other ligands, is that the levels may be higher than those in pathophysiological states. Studies using systemic Wnt/β-catenin inhibitors are useful for therapeutic investigation but do not elucidate the cell-specific roles of this pathway in injury. Several studies have used ICG-001 as a Wnt/β-catenin inhibitor, but this compound actually blocks the NH_2 terminus of cyclic AMP response element–binding protein (CBP), which inhibits β-catenin/TCF–mediated transcription (44). As recently shown in immune cells, ICG-001 does not completely block all β-catenin signaling but rather β-catenin/TCF–dependent signaling (36). Another concern with ICG-001 is that it can inhibit signaling pathways other than β-catenin that are dependent upon binding to the amino terminus of CBP.

Stabilizing β-catenin in PTs using *Ggt-Cre* was beneficial in 2 models of AKI to CKD progression. One question about this genetic model is whether the deletion of exon 3 negatively affects β-catenin binding to TCF/LEF or artificially augments binding to FoxO3. In Supplemental Figure 1, we show that β-catenin signaling with TCF/LEF is augmented in the conditional β-catenin–stabilized mouse using the Topflash reporter mice and *Axin2* expression, both of which depend upon TCF/LEF binding, without renal injury

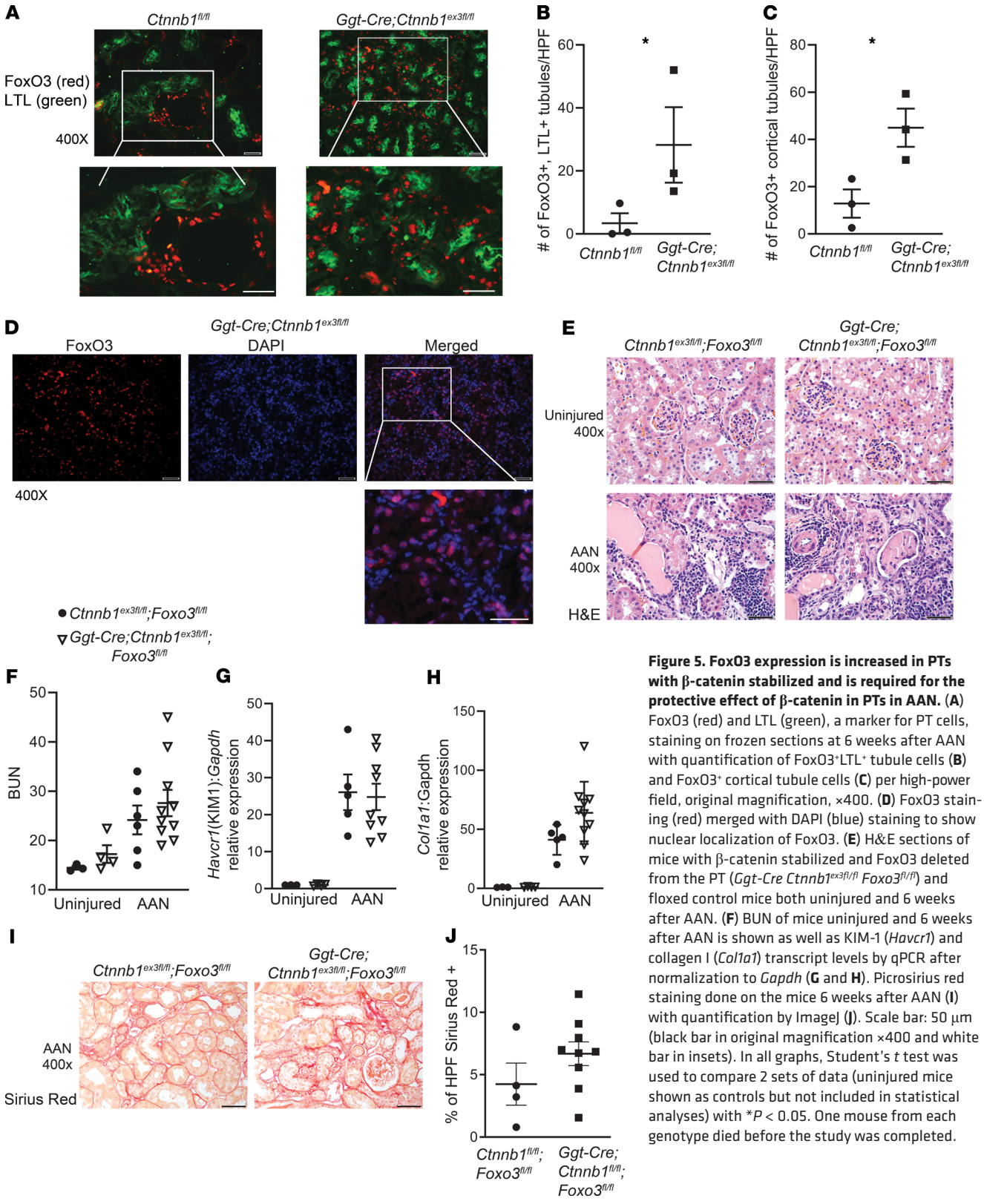

Figure 5. FoxO3 expression is increased in PTs with β-catenin stabilized and is required for the protective effect of β-catenin in PTs in AAN. (**A**) FoxO3 (red) and LTL (green), a marker for PT cells, staining on frozen sections at 6 weeks after AAN with quantification of FoxO3$^+$LTL$^+$ tubule cells (**B**) and FoxO3$^+$ cortical tubule cells (**C**) per high-power field, original magnification, ×400. (**D**) FoxO3 staining (red) merged with DAPI (blue) staining to show nuclear localization of FoxO3. (**E**) H&E sections of mice with β-catenin stabilized and FoxO3 deleted from the PT (*Ggt-Cre Ctnnb1*$^{ex3fl/fl}$ *Foxo3*$^{fl/fl}$) and floxed control mice both uninjured and 6 weeks after AAN. (**F**) BUN of mice uninjured and 6 weeks after AAN is shown as well as KIM-1 (*Havcr1*) and collagen I (*Col1a1*) transcript levels by qPCR after normalization to *Gapdh* (**G** and **H**). Picrosirius red staining done on the mice 6 weeks after AAN (**I**) with quantification by ImageJ (**J**). Scale bar: 50 μm (black bar in original magnification ×400 and white bar in insets). In all graphs, Student's *t* test was used to compare 2 sets of data (uninjured mice shown as controls but not included in statistical analyses) with $^*P < 0.05$. One mouse from each genotype died before the study was completed.

(i.e., oxidative stress), indicating that β-catenin binding to TCF/LEF is intact. Although we cannot definitively rule out the possibility that exon 3 deletion enhances β-catenin binding to FoxO3, the location of exon 3 (NH_2 terminal region of β-catenin) (24, 45) is distinct from the central armadillo repeat region of β-catenin, which is the binding site of FoxO3 (32). In addition, our in vitro studies show that β-catenin

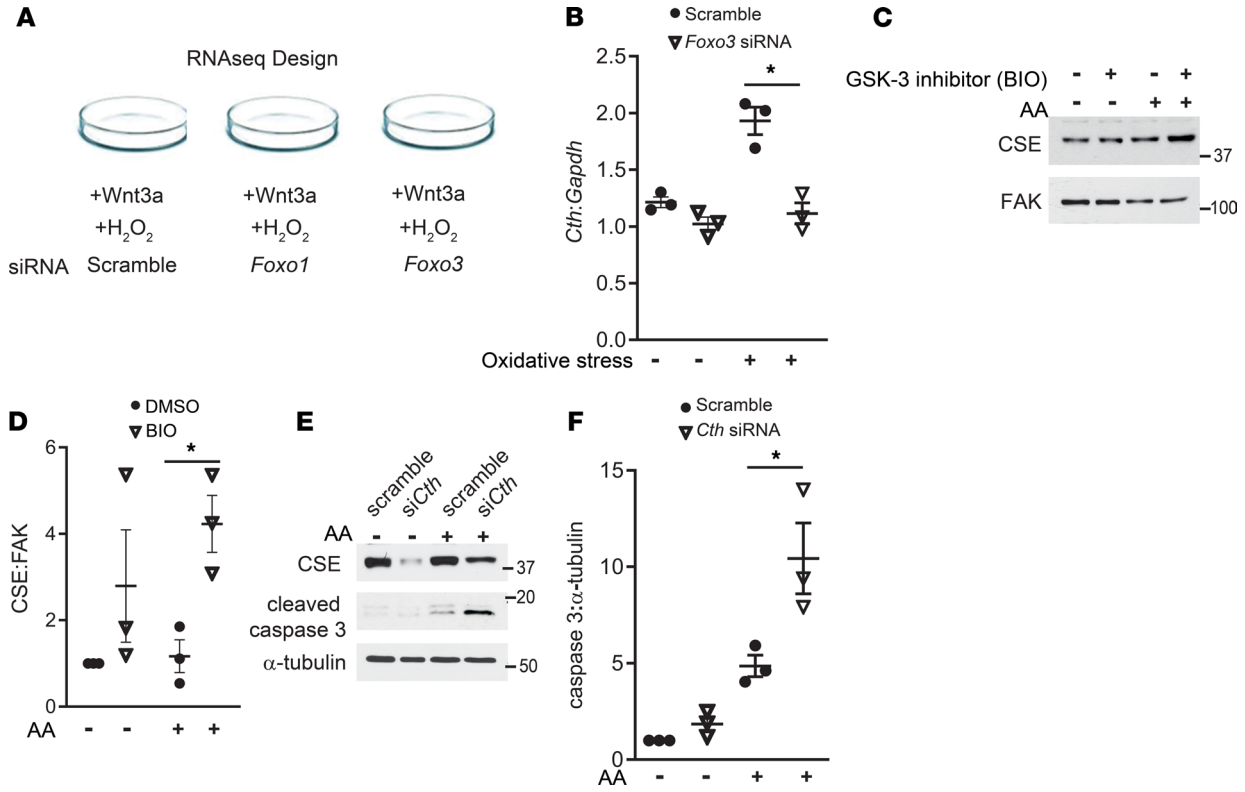

Figure 6. CSE identified as a potentially novel target of β-catenin and FoxO3 in PT cells. (**A**) RNA-Seq was performed on PT cells transfected with *Foxo1*, *Foxo3*, or scramble siRNA, treated with Wnt3a 20 ng/mL and H_2O_2 100 μM in serum-free medium for 16 hours. (**B**) *Cth*, the gene for CSE, was validated as a target for β-catenin and FoxO3 using PT cells. The cells were transfected with *Foxo3* or scramble siRNA, then treated with Wnt3a (20 ng/mL) in the presence or absence of oxidative stress (100 μM H_2O_2 in serum-free medium) for 24 hours, and *Cth* transcripts were measured by qPCR and normalized to *Gapdh* (**B**). *$P < 0.05$ using the Student's *t* test. (**C**) PT cells were treated ± AA at 30 μM for 7 days with a GSK-3 inhibitor added for the last 2 days, and protein lysates were immunoblotted for CSE with FAK for loading control and quantified using ImageJ (**D**). PT cells were transfected with either *Cth* or scramble siRNA and then treated ± AA. (**E**) Effective reduction in CSE was verified with immunoblots and cleaved caspase-3 measured to detect apoptosis with α-tubulin for loading control. Immunoblots were quantified from 3 independent experiments using ImageJ (**F**). The statistics for RNA-Seq are discussed in the Methods. For all other comparisons, the Student's *t* test comparing 2 sets of data was used (cells without oxidative stress or AA are shown as controls but not included in analyses) with *$P < 0.05$.

binding to FoxO3 is enhanced in oxidative stress independent of the exon 3 mutation. Thus, there is no evidence that the conditionally β-catenin–stabilized mouse has impaired TCF/LEF binding, and it is unlikely, though not impossible, that FoxO3 binding is altered by exon 3 deletion.

Mice with conditional β-catenin stabilization had less epithelial injury as evidenced by preserved BUN and lower KIM-1 levels in both the AA and IRI models. Furthermore, the conditionally stabilized mice had increased LTL expression after IRI, indicating more differentiated PTs with brush border intact (29). There was protection against fibrosis in the AA model in which collagen expression and sirius red staining were significantly attenuated, whereas there was only a nonsignificant trend toward improvement in collagen ($P = 0.06$) and sirius red (data not shown) in the IRI model. This is partly explained by the difference in injury severity because the AA-treated floxed control mice had higher BUN levels 6 weeks later than did the IRI floxed controls. Both injuries target the PTs, causing direct and chronic tubular injury, which can lead to progressive CKD. Injury to the PTs is sufficient to cause fibrosis (4), but this is likely an indirect effect caused by paracrine signaling from injured tubules to neighboring myofibroblasts. From these models, one may conclude that epithelial β-catenin plays a stronger role in tubular survival and renal function than in renal fibrosis.

The AA model causes acute proximal tubular injury, which then progresses to chronic tubule damage and interstitial fibrosis. Continued tubular apoptosis/necrosis was detected even 6 weeks after injury based upon $TUNEL^+$ tubule cells. Thus, we used an AA in vitro model of cell death to further explore the mechanisms of chronic injury. Treating PT cells with AA for 7 days is longer than most in vitro apoptotic stimuli though not a perfect mimic of the in vivo environment. Both FoxO3 and CSE protected PT cells from apoptosis in this in vitro model of AA. The relationship between tubular apoptosis and fibrosis requires

Table 1. Genes with altered expression in proximal tubule cells treated with Wnt3a and oxidative stress

Genes suppressed by *Foxo3* siRNA	Genes augmented by *Foxo3* siRNA
Ctgf	Aqp1
Aldh1l2	*Aldh1a7*
Gadd45g	*Cd55*
Cth	*Olfm1*
Oasl2	*Plat*
Ccl17	*Ces2e*
Adgrg1	*Aldh1a1*
Foxj1	
Ifit1	
Serpine1	
Dhrs3	
Col4a4	

further research, but several studies have linked ongoing epithelial cell death to CKD progression in both human and rodent injured kidneys (46–51). Others have reported that β-catenin signaling may promote epithelial survival in AKI, but the dogma has been that prolonged β-catenin signaling would be detrimental in the context of CKD. Our data indicate that β-catenin/FoxO3 interactions in oxidative stress promote epithelial survival, potentially through the novel target CSE.

To our knowledge, this is the first study to increase β-catenin signaling specifically in PT cells. Another group stabilized β-catenin in tubules using the Ksp-Cre mouse model, which targets distal tubules more than PTs (52). They used a protein overload model of injury and did not observe differences in fibrosis but did report augmented inflammation in the Ksp-Cre mice. The differences in responses may be due to different tubule compartments being targeted and/or different amounts of β-catenin signaling. The distal tubule is known to have greater basal β-catenin signaling (6), and it is possible that augmenting this pathway above a certain amount is deleterious. This idea of a dose-dependent response or therapeutic window has support in both the developing kidney and the podocyte, where too little or too much β-catenin signaling was detrimental (7, 53). Our RNA-Seq data revealed several mediators of inflammation (e.g., *Ctgf*, *Ccl18*, *Foxj1*, *Adgrg1*) that were suppressed with *Foxo3* siRNA. Thus, at higher levels of β-catenin activity as might be seen in distal tubules, these inflammatory effects may outweigh any antiapoptotic or antioxidant beneficial effects.

Interactions between β-catenin and FoxO transcription factors have been studied in the context of diabetes, cancer, aging, and bone formation (54–56). The specific effects of β-catenin/FoxO interactions vary depending upon the microenvironment, and the downstream mediators of these effects have not been well characterized. To our knowledge, our group is the first to investigate how oxidative stress–dependent β-catenin and FoxO3 interactions affect epithelial injury. Recently, another group showed that giving mice recombinant TGF-β and the ICG-001 inhibitor in models of renal fibrosis led to greater regulatory T cell (Treg) differentiation and less inflammation (36). This phenotype was thought to be due to beneficial actions of β-catenin and FoxO1 in promoting Tregs, thus suggesting that these interactions may be beneficial in cells other than PTs. Consistent with our data, this same group showed that FoxO1 protected murine kidney tubular cells from TGF-β–induced profibrotic protein expression in vitro (57). Surprisingly, oxidative stress alone reduced nuclear β-catenin (Figure 3F). Others have published that H_2O_2 reduces β-catenin signaling in endothelial cells through impaired miRNA-154, which inhibits dickkopf-related protein 2, an inhibitor of Wnt/β-catenin signaling (58). However, more research is necessary to determine whether this mechanism applies to renal tubules.

Our data suggest that FoxO3 is necessary for proximal tubular β-catenin-mediated protection in chronic injury because the mice with β-catenin stabilized but lacking FoxO3 lost their protective effect. FoxO transcription factors are known to have effects on antioxidant production, cell survival/apoptosis, and cell cycle. Conflicting reports exist about how these biological responses are affected, and there are numerous posttranslational modifications that can alter FoxO activity, perhaps accounting for its diverse context-dependent effects. This raises the critical question of what the transcriptional targets are that mediate

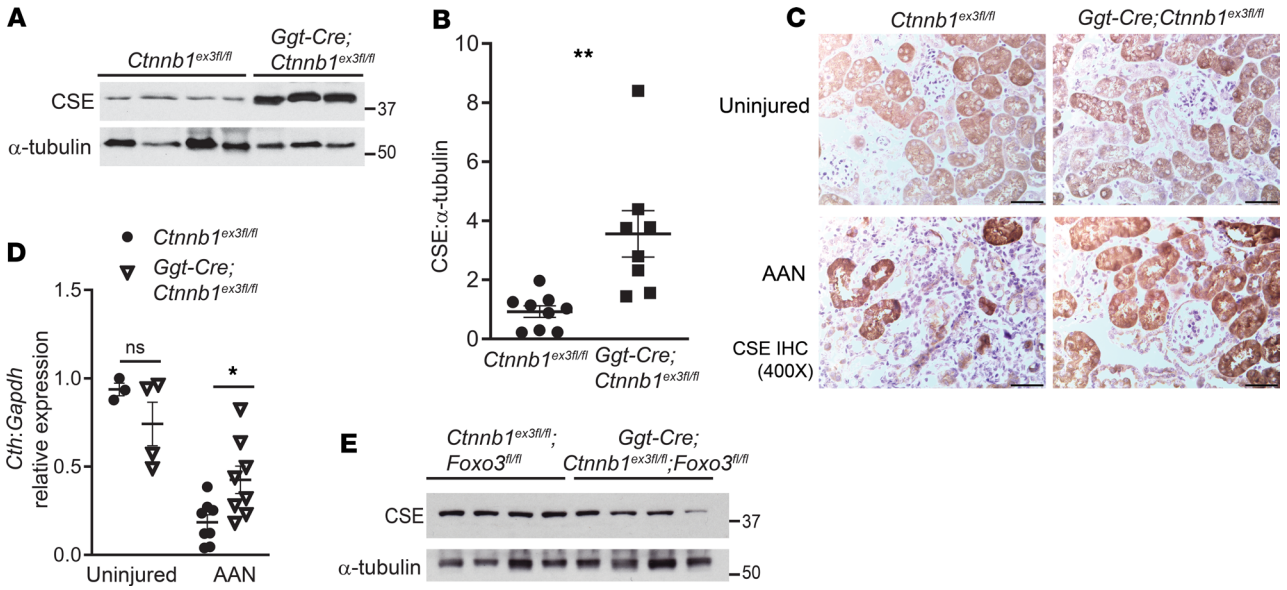

Figure 7. Injured mice with β-catenin stabilized in the PT have increased protein expression of CSE. (**A**) Cortical lysates from *Ggt-Cre Ctnnb1*$^{ex3fl/fl}$ mice and floxed controls 6 weeks after AA treatment were immunoblotted for CSE with α-tubulin for loading control. (**B**) ImageJ was used to quantify the differences in CSE protein expression. (**C**) Immunohistochemistry for CSE was performed on uninjured and AAN (6 weeks) kidneys. (**D**) *Cth* transcripts were measured by qPCR in renal cortical tissue from uninjured and 6-week AA-treated mice. (**E**) Immunoblots from cortical lysates of mice injured by AA and stained for CSE and α-tubulin for loading control. Student's *t* test was used to compare 2 groups of samples with $^*P < 0.05$ and $^{**}P < 0.01$. Scale bar: 50 μm.

these β-catenin/FoxO–dependent responses in the chronically injured kidney. We identified under 20 genes that were either up- or downregulated in *Foxo3*-siRNA–treated PT cells under conditions of oxidative stress and β-catenin activation (Table 1). We focused on CSE since this enzyme can reduce injury of the kidney and other organs and has not, to our knowledge, been identified as a downstream target of β-catenin/FoxO3 (41, 59). It is possible that β-catenin/FoxO3 directly target a different gene, which then modulates *Cth* transcription. Our studies did not determine whether β-catenin/FoxO3 directly or indirectly upregulate *Cth* gene expression in oxidative stress.

CSE is 1 of 3 enzymes involved in H_2S generation, and CSE expression has been localized to the PTs, consistent with our immunohistochemistry data (60). H_2S, like nitric oxide and carbon monoxide, is a gasotransmitter that is toxic at high doses, but at lower doses it acts as a signaling molecule to regulate biological processes, such as vascular tone and inflammation. Augmentation of H_2S, generally from exogenous Na_2S or NaHS, may promote cell survival through modulation of caspase activity and may be antiinflammatory through NF-κB inhibition (61). Although we show that CSE has an antiapoptotic effect on PT cells in vitro and others have shown that H_2S protects against CKD by reducing apoptosis in murine kidneys (40), there are other mechanisms whereby CSE may be beneficial. CSE, through the generation of cysteine from cystathionine, contributes to the synthesis of the antioxidant glutathione (Figure 8). H_2S also inhibits reactive oxygen species (ROS) production by the mitochondria, blocks glucose-induced NADPH oxidase 4, and scavenges ROS (39, 62, 63). Thus, CSE/H_2S may be protective in injury through blocking apoptosis, inflammation, or oxidative stress. It was recently reported that FoxO3 is protective in injured renal tubules through effects on autophagy and oxidative stress (64). Although there are likely multiple FoxO3 targets, it may be that FoxO3-dependent cell survival and antioxidant function are mediated, in part, through CSE.

This novel β-catenin/FoxO3/CSE pathway in PTs has important clinical implications for CKD. Because many reports describe the profibrotic actions of β-catenin, particularly in the tubulointerstitium, our data should give pause to blocking this pathway given the beneficial effects on the PT. There have been concerns that sustained β-catenin signaling in the PTs would be detrimental, but our data suggest otherwise and that the location of β-catenin signaling is more important than the duration. Consistent with this, fibroblast-specific β-catenin signaling is detrimental even in AKI (65), a process in which β-catenin signaling is widely considered to be beneficial. Human diabetic nephropathy biopsies show altered β-catenin and FoxO1/3 gene expression profiles, but targeting these transcription factors may be problematic

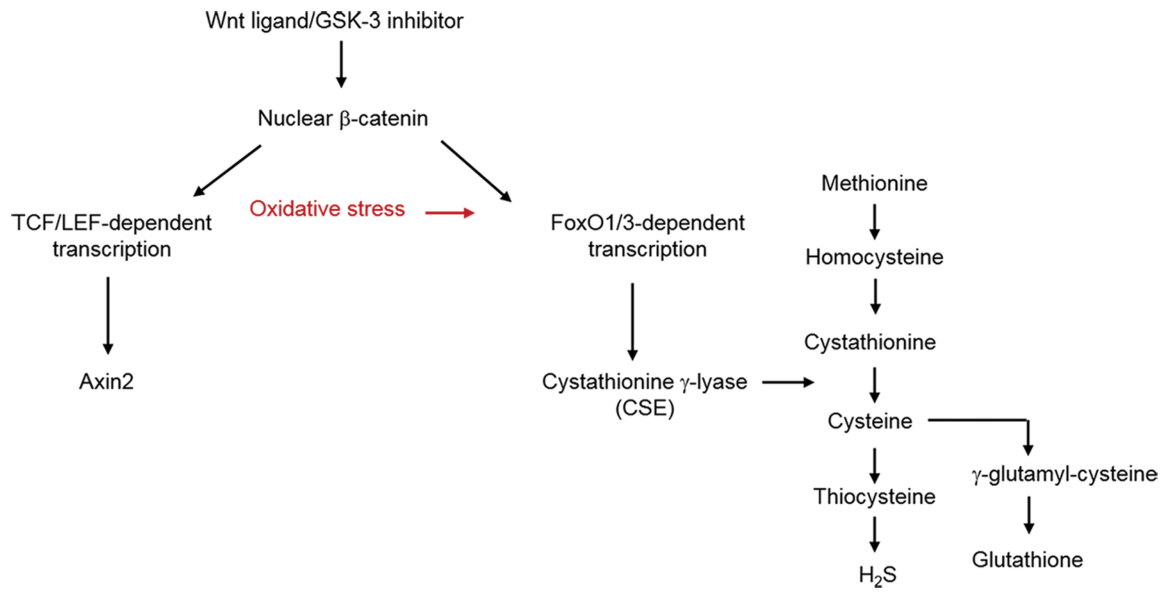

Figure 8. Schematic of how oxidative stress modulates β-catenin and FoxO signaling to affect H_2S and glutathione through CSE. Wnt ligands and GSK-3 inhibitors both rescue β-catenin from degradation leading to increased nuclear (i.e., transcriptionally active) β-catenin. Usually β-catenin partners with transcription factors TCF/LEF, but in oxidative stress, β-catenin promotes FoxO1/3-dependent activity. One downstream target of β-catenin and FoxO3 is CSE, which converts cystathionine to cysteine and contributes to H_2S and glutathione production.

given their target-specific actions unless a site-specific approach is feasible (66, 67). Given the beneficial preclinical data on CSE/H_2S in CKD (40, 41, 68) and the reduced H_2S expression in the plasma of hemodialysis patients (69), this downstream target of Wnt/β-catenin may have greater therapeutic promise.

Methods

Animal models. Mice with a conditional activating mutation of β-catenin in which exon 3 of Ctnnb1 is floxed (*Ctnnb1*$^{ex3fl/fl}$) were produced in-house (Kyoto University) (24). Floxed *Foxo3* (*Foxo3*$^{fl/fl}$) mice were obtained from Jackson Laboratory. Mice expressing Cre recombinase under the control of *Ggt* promoter (*Ggt-Cre*) were a gift from Eric Neilson (Vanderbilt University) but are also available at The Jackson Laboratory and have been previously characterized (30). Wnt/β-catenin reporter or Topflash (*Tcf/Lef:H2B-GFP*) mice harboring H2B-EGFP fusion protein expression under the control of TCF/LEF1 response element (26) were obtained from The Jackson Laboratory. We used male mice 8–12 weeks old for all injury models. The *Ggt-Cre Ctnnb1*$^{ex3fl/fl}$ mice were N10 on BALB/c background whereas the other genotypes were on mixed backgrounds.

Injury models. For the AAN model, all mice received intraperitoneal injections of aristolochic acid (AAI, MilliporeSigma) every other day for 2 weeks for a total of 6 injections and were euthanized 6 weeks after the last injection unless stated otherwise. *Ggt-Cre Ctnnb1*$^{ex3fl/fl}$ and floxed WT mice were given 4.5 mg/kg AA per injection, and *Ggt-Cre Ctnnb1*$^{ex3fl/fl}$ *Foxo3*$^{fl/fl}$ mice groups received 6 mg/kg. IRI was carried out as previously described (70). Briefly, mice were anesthetized with ketamine/xylazine and maintained on a 37°C heat pad during surgery. The left kidney was exposed via a flank incision, and the renal pedicle was clamped for 30 minutes. Eight days later, the contralateral kidney was removed, and the mice were sacrificed 4 weeks after the initial unilateral IRI.

Tissue staining and injury score. Kidneys were harvested, fixed in 4% paraformaldehyde, paraffin-embedded, and stained with H&E and TUNEL as previously described (71) or picrosirius red. For quantification of TUNEL staining, 10–15 high-power fields (original magnification, ×400) were taken per sample, and the number of cortical tubules with TUNEL$^+$ nuclei was counted. For picrosirius red, 10 high-power fields of kidney cortex were taken per sample, and quantification of the area staining red was done using ImageJ (NIH). Colleagues in renal pathology scored renal injury from nonoverlapping fields in the cortex (original magnification, ×200) using the following system for renal injury: 0= no injury, 1 = 1%–20% of area, 2 = 21%–50% of area, 3 = 51%–75% of area, and 4 = >75%. Tubular injury was defined as tubular sloughing, cast formation, dilatation, degeneration, atrophy, or tubulitis. In all cases, the investigator taking the pictures and counting the nuclei or quantifying the staining or histology did so unaware of the animals' genotypes.

Tissue immunohistochemistry and fluorescence. Paraffin-embedded tissues were rehydrated with decreasing concentrations of ethanol, and antigen target retrieval was performed with 100 mM Tris buffer (pH 10) in a pressure cooker. The antigen/antibody complexes were detected with biotinylated secondary antibody (BA-1000 Vector Laboratories), amplified with ABC Elite peroxidase (Vector Laboratories), and detected by DAB (MilliporeSigma). For immunofluorescence, the antigen retrieval treatments on paraffin-embedded and OCT-embedded frozen tissues were performed using proteinase K (MilliporeSigma) at 37°C and 10 mM citrate buffer (pH 7.2) at 56°C, respectively. Rehydrated tissue sections were incubated with 1:400 LTL with FITC conjugated (Vector Laboratories) in PBS containing Ca^+/Mg^+ after blocking with 5% BSA. LTL^+ area was quantified in ×200 fields (5 fields/sample) using ImageJ. Immunofluorescent images were taken with an Olympus BX51, and all others were taken using a Nikon Eclipse E600 microscope.

Renal function. Blood from the tail vein was collected from injured mice at the time of euthanasia, placed in heparinized tubes, and centrifuged and the plasma supernatant used with the Thermo Infinity Urea Reagent to determine BUN levels.

Subcellular fractionation using renal cortices. Nuclear and cytosolic fractionation were performed as previously described (72). Briefly, uninjured renal cortices were grossly dissected and minced in a Petri dish using cold PBS with protease inhibitors (MilliporeSigma), resuspended in ice-cold buffer (250 mM sucrose, 50 mM Tris-HCl pH 7.4, 5 mM $MgCl_2$, 1 mM DTT, 25 μg/mL spermine, 25 μg/mL spermidine, and protease inhibitors), homogenized, and centrifuged at 800 *g* for 15 minutes to yield the whole cytosolic fraction (supernatants) and the nuclear fractions (pellets). The pellets were solubilized in 2 M sucrose, 50 mM Tris-HCl pH 7.4, 5 mM $MgCl_2$, 1 mM DTT, 25 μg/mL spermine, 25 μg/mL spermidine, and protease inhibitors; filtered; and centrifuged in a swing-bucket ultracentrifuge at 80,000 *g* for 35 minutes. The pellets, pure nuclei, were resuspended in NE buffer (20 mM HEPES pH 7.9, 1.5 mM $MgCl_2$, 0.5 M NaCl, 0.2 mM EDTA, 20% glycerol, 1% Triton X-100, 1 mM DTT, and protease and phosphatase inhibitors) and centrifuged 30 minutes at 9000 *g*. The supernatants were saved as soluble nuclear proteins while the pellets, constituted of DNA tightly bound proteins, were resuspended in RIPA buffer.

Subcellular fractionation using PT cells. Nuclear and cytoplasmic cell fractionation were performed as previously described (35). Briefly, PT cells were lysed with a hypotonic lysis buffer (10 mM HEPES pH 7.8, 10 mM KCl, 2 mM $MgCl_2$, 0.1 mM EDTA, with protease and phosphatase inhibitors), then centrifuged for 2 minutes at 16,000 *g* to separate the cytoplasmic fraction (supernatant) from the nuclear compartment (pellet). The pellet was then resuspended in a hypertonic buffer (50 mM HEPES pH 7.8, 50 mM KCl, 300 mM NaCl, 0.1 mM EDTA, 10% glycerol with protease and phosphatase inhibitors) and centrifuged for 30 seconds at 3000 *g* twice to extract pure nuclei (pellets), which were resuspended in RIPA buffer.

Cell culture. Conditionally immortalized and thermolabile PT cells were generated from the Immorto-mouse as previously described and characterized (30). These PT cells had the TGF-β receptor floxed, but the receptor was still intact and TGF-β signaling was not impaired. PT cells were grown at 33°C in DMEM/F12 supplemented with 2.5% fetal bovine serum, hydrocortisone, insulin, transferrin, selenium, triiodothyronine, and penicillin/streptomycin (complete PT medium) with interferon-γ. Before experiments, PT cells were moved to 37°C, and interferon-γ was removed to induce differentiation. Primary cell cultures were generated as previously described with some modifications (73). Briefly, renal cortices were digested in collagenase I (1 mg/mL) and dispase (1 mg/mL) with DNAse, passed through a 70-μm filter to remove glomeruli, washed with complete PT medium, and plated in RPMI 1640 medium (Corning) supplemented with 10% FBS, then reduced to 5% FBS, 1 mM glucose, and supplements listed above for complete PT medium.

Generation of PT cells with Topflash luciferase reporter. PT cells were incubated with complete PT medium plus 1 mL of lentivirus containing the Topflash/luciferase construct and polybrene or the empty vector for 6 hours at 37°C. PT cells were then replaced with complete PT medium with interferon-γ and moved to 33°C. Cells were incubated with 0.5 μg/mL of puromycin to select infected cells for 1 week. Afterward, cells were cultured in complete PT medium. Lentiviral transduction and Topflash activity were confirmed by luciferase assay after stimulating cells with Wnt3a (Time Bioscience).

Cell experiments with AA, H_2O_2, and reagents. PT cells were plated at 30% confluence in complete PT medium containing 20 μM of AA (unless otherwise specified) for 7 days. For some experiments, the GSK-3 inhibitor BIO (MilliporeSigma) or Wnt3a was added at 500 nM and 10 ng/mL, respectively, unless another dose is mentioned, or an equal volume of diluent while being treated with AA. Cells were treated 24 hours with 100 μM H_2O_2 to generate oxidative stress.

siRNA. PT cells were transfected with siRNA targeted to FoxO1, FoxO3, or scramble using Silencer Pre-Designed and Validated sequences from Ambion (siRNA ID s80659, s80621; Thermo Fisher Scientific) or a pool of 2 siRNA duplexes to Cth (CSE) from Santa Cruz Biotechnology (sc-142618). Cells were transfected in OptiMEM using lipofectamine RNAiMax (Thermo Fisher Scientific).

PCR. RNA was extracted from tissue and from cells using the QIAGEN RNeasy Mini Kit, and Bio-Rad's iScript cDNA Synthesis Kit generated cDNA. For RNA extraction, PT cells were directly lysed with RLT buffer (QIAGEN) while renal cortices were mechanically disrupted in Lysis Matrix Tubes (MP Biomedicals) containing the lysis buffer (RLT) supplemented with 1% β-mercaptoethanol before being purified on the silica membrane RNeasy spin columns. Quantitative real-time PCR was performed with 25–100 ng cDNA and iQ SYBR Green Supermix using the Bio-Rad CFX96 thermal cycler. Relative mRNA expressions were determined by ΔΔCT equation, and, after validation with a panel of housekeeping genes, *Gapdh* was used as a reference gene. Primer sequences are as follows (forward and reverse): *Gapdh* 5′-AGGTCGGTGTGAACGGATTTG-3′ and 5′-TGTAGACCATGTAGTTGAGGTCA-3′, *Havcr1* (KIM-1) 5′-CTCTAAGCGTGGTTGCCTTC-3′ and 5′-GGGCCACTGGTACTCATTCT-3′, *Col1a1* 5′-GGGTCTAGACATGTTCAGCTTTGTG-3′ and 5′-ACCCTTAGGCCATTGTGTATGC-3′, *Axin2* 5′-TGAGCTGGTTGTCACCTACT-3′ and 5′- CACTGTCTCGTCGTCCCA-3′, and *Cth* 5′-CCCAGGGATGGTCAGTTTCT-3 and 5′-TCATTGATCCCGAGGGTAGC-3′.

RNA-Seq analysis. PT cells were treated with siRNA to *Foxo1*, *Foxo3*, *Foxo1/3*, or scramble; exposed to oxidative stress using 100 μM H_2O_2 in serum-free medium; and treated with Wnt3a to activate β-catenin. RNA-Seq was performed by the VUMC Core Vanderbilt Technologies for Advanced Genomics using the Illumina HiSeq 2500. Data analysis was performed by the VUMC Core Vanderbilt Technologies for Advanced Genomics Analysis and Research Design, and the RNA-Seq data were quality controlled following the multiperspective guideline (74). Quality control metrics were computed from software QC3 (75), and no quality issues were observed. Alignment was performed by TopHat 2 (76) on MM10 mouse reference genome followed by gene quantification into fragments per kilobase million using Cufflinks (77). Differential expression analyses were performed using cuffdiff from the Cufflinks package. *P* values were adjusted using the Benjamini-Hochberg method. These data have been uploaded to the National Center for Biotechnology Information's Gene Expression Omnibus database and can be accessed through record GSE144915.

Immunoblots and reagents. Cells were lysed using MilliporeSigma's Mammalian Lysis Buffer plus protease and phosphatase inhibitors, sheared using an insulin syringe, clarified by centrifugation, and quantified using the BCA protein assay (Thermo Fisher Scientific). Tissue lysates were generated as described in the subcellular fractionation sections. Both cell and tissue proteins were separated by SDS-PAGE and incubated with the following primary antibodies from Cell Signaling Technology: β-catenin (9587S), cleaved caspase-3 (9664S/5A1E), α-tubulin (3873S/DM1A), histone H3 (3638/96C10), and FoxO3 (12829/D19A7); Santa Cruz Biotechnology: nitrotyrosine (sc-32757/39B6) and FAK (sc-558, C-20); Abcam: cystathionase (ab151769); and Vector Laboratories: LTL (FL-1321). ImageJ software was used to quantify bands on autoradiography film.

Nuclear coimmunoprecipitation. Nuclear protein fractions were isolated as described above. Proteins interacting with β-catenin were pulled down using β-catenin antibody (Cell Signaling Technology) or IgG control and protein A agarose beads (Pierce Biotechnology, Thermo Fisher Scientific). After multiple washes in IP buffer (25 mM Tris, 150 mM NaCl; pH 7.2 with protease inhibitors), proteins were eluted, denatured, and probed with FoxO3 antibody.

Statistics. We used the 2-tailed Student's *t* test with unequal variance to compare 2 sets of data, with $P < 0.05$ considered statistically significant. The 1-way ANOVA was used for experiments in which there were multiple comparisons. All experiments subject to analysis were performed at least 3 times. Quantitative data graphs are shown as dot plots with the mean ± SEM.

Study approval. All procedures were approved by the Institutional Animal Care and Use Committee of VUMC and conducted according to the NIH's *Guide for the Care and Use of Laboratory Animals* (National Academies Press, 2011).

Author contributions

SNK began the project, which was finished by YO, and both performed experiments in vivo and in vitro and helped in the writing and editing of the manuscript. LS performed the IRI experiments; MPM did all the mouse colony maintenance and genotyping. JT, KSD, SN, AI, TH, and RM performed experiments,

analyzed data, and edited the manuscript. HY did the histologic scoring, and MMT, MD, BK, RCH, and EL helped with key reagents, experimental design, and editing of the manuscript. LSG conceived of the project, oversaw the experiments, and wrote and edited the manuscript.

Acknowledgments

This work was supported by NIH grants R01-DK-108968-01 (LG), DK51265 (RCH), R35GM122516 (EL), 1R01DK112688 (MD), and W81XWH-17-1-0610 (MD); Vanderbilt O'Brien Kidney Center NIH grant 1-P30-DK-114809-01 (LG); Swiss National Science Foundation; Ambizione grant PZ00P3_179916 (SNK); and the Vanderbilt Center for Kidney Disease, Department of Veterans Affairs, Veterans Health Administration VA Merit Awards 1I01BX003425-01A1 (LG), 00507969 (RCH), and I01BX001340 (BK).

Address correspondence to: Leslie Gewin, Room S3304 MCN, 1161 21st Avenue South, Vanderbilt University Medical Center, Nashville, Tennessee 37232, USA. Phone: 615.343.0767; Email: l.gewin@vumc.org.

1. United States Renal Data System. *2016 USRDS Annual Data Report: Epidemiology of Kidney Disease in the United States*. Bethesda, Maryland, USA: National Institutes of Health, National Institute of Diabetes and Digestive and Kidney Diseases; 2016.
2. Hill NR, et al. Global prevalence of chronic kidney disease - a systematic review and meta-analysis. *PLoS One*. 2016;11(7):e0158765.
3. Coca SG, Singanamala S, Parikh CR. Chronic kidney disease after acute kidney injury: a systematic review and meta-analysis. *Kidney Int*. 2012;81(5):442–448.
4. Grgic I, et al. Targeted proximal tubule injury triggers interstitial fibrosis and glomerulosclerosis. *Kidney Int*. 2012;82(2):172–183.
5. Takaori K, et al. Severity and frequency of proximal tubule injury determines renal prognosis. *J Am Soc Nephrol*. 2016;27(8):2393–2406.
6. Kawakami T, Ren S, Duffield JS. Wnt signalling in kidney diseases: dual roles in renal injury and repair. *J Pathol*. 2013;229(2):221–231.
7. Marose TD, Merkel CE, McMahon AP, Carroll TJ. Beta-catenin is necessary to keep cells of ureteric bud/Wolffian duct epithelium in a precursor state. *Dev Biol*. 2008;314(1):112–126.
8. Bridgewater D, et al. Canonical WNT/beta-catenin signaling is required for ureteric branching. *Dev Biol*. 2008;317(1):83–94.
9. Clevers H, Nusse R. Wnt/β-catenin signaling and disease. *Cell*. 2012;149(6):1192–1205.
10. Terada Y, et al. Expression and function of the developmental gene Wnt-4 during experimental acute renal failure in rats. *J Am Soc Nephrol*. 2003;14(5):1223–1233.
11. Lin SL, et al. Macrophage Wnt7b is critical for kidney repair and regeneration. *Proc Natl Acad Sci U S A*. 2010;107(9):4194–4199.
12. He W, Dai C, Li Y, Zeng G, Monga SP, Liu Y. Wnt/beta-catenin signaling promotes renal interstitial fibrosis. *J Am Soc Nephrol*. 2009;20(4):765–776.
13. Zhou D, Li Y, Lin L, Zhou L, Igarashi P, Liu Y. Tubule-specific ablation of endogenous β-catenin aggravates acute kidney injury in mice. *Kidney Int*. 2012;82(5):537–547.
14. Wang Z, Havasi A, Gall JM, Mao H, Schwartz JH, Borkan SC. Beta-catenin promotes survival of renal epithelial cells by inhibiting Bax. *J Am Soc Nephrol*. 2009;20(9):1919–1928.
15. Howard C, et al. Specific deletion of glycogen synthase kinase-3β in the renal proximal tubule protects against acute nephrotoxic injury in mice. *Kidney Int*. 2012;82(9):1000–1009.
16. Luo C, et al. Wnt9a promotes renal fibrosis by accelerating cellular senescence in tubular epithelial cells. *J Am Soc Nephrol*. 2018;29(4):1238–1256.
17. Maarouf OH, et al. Paracrine Wnt1 drives interstitial fibrosis without inflammation by tubulointerstitial cross-talk. *J Am Soc Nephrol*. 2016;27(3):781–790.
18. Madan B, et al. Experimental inhibition of porcupine-mediated Wnt O-acylation attenuates kidney fibrosis. *Kidney Int*. 2016;89(5):1062–1074.
19. Xiao L, et al. Sustained activation of Wnt/β-catenin signaling drives AKI to CKD progression. *J Am Soc Nephrol*. 2016;27(6):1727–1740.
20. Kim K, Lu Z, Hay ED. Direct evidence for a role of beta-catenin/LEF-1 signaling pathway in induction of EMT. *Cell Biol Int*. 2002;26(5):463–476.
21. Grande MT, et al. Snail1-induced partial epithelial-to-mesenchymal transition drives renal fibrosis in mice and can be targeted to reverse established disease. *Nat Med*. 2015;21(9):989–997.
22. Maiese K, Hou J, Chong ZZ, Shang YC. A fork in the path: developing therapeutic inroads with FoxO proteins. *Oxid Med Cell Longev*. 2009;2(3):119–129.
23. Iwano M, Plieth D, Danoff TM, Xue C, Okada H, Neilson EG. Evidence that fibroblasts derive from epithelium during tissue fibrosis. *J Clin Invest*. 2002;110(3):341–350.
24. Harada N, et al. Intestinal polyposis in mice with a dominant stable mutation of the beta-catenin gene. *EMBO J*. 1999;18(21):5931–5942.
25. Jho EH, Zhang T, Domon C, Joo CK, Freund JN, Costantini F. Wnt/beta-catenin/Tcf signaling induces the transcription of Axin2, a negative regulator of the signaling pathway. *Mol Cell Biol*. 2002;22(4):1172–1183.
26. Ferrer-Vaquer A, Piliszek A, Tian G, Aho RJ, Dufort D, Hadjantonakis AK. A sensitive and bright single-cell resolution live imaging reporter of Wnt/ß-catenin signaling in the mouse. *BMC Dev Biol*. 2010;10:121.
27. Neelisetty S, et al. Renal fibrosis is not reduced by blocking transforming growth factor-β signaling in matrix-producing intersti-

tial cells. *Kidney Int*. 2015;88(3):503–514.
28. Huang L, Scarpellini A, Funck M, Verderio EA, Johnson TS. Development of a chronic kidney disease model in C57BL/6 mice with relevance to human pathology. *Nephron Extra*. 2013;3(1):12–29.
29. Kusaba T, Lalli M, Kramann R, Kobayashi A, Humphreys BD. Differentiated kidney epithelial cells repair injured proximal tubule. *Proc Natl Acad Sci U S A*. 2014;111(4):1527–1532.
30. Gewin L, et al. Deleting the TGF-β receptor attenuates acute proximal tubule injury. *J Am Soc Nephrol*. 2012;23(12):2001–2011.
31. Saito S, Tampe B, Müller GA, Zeisberg M. Primary cilia modulate balance of canonical and non-canonical Wnt signaling responses in the injured kidney. *Fibrogenesis Tissue Repair*. 2015;8:6.
32. Essers MA, de Vries-Smits LM, Barker N, Polderman PE, Burgering BM, Korswagen HC. Functional interaction between beta-catenin and FOXO in oxidative stress signaling. *Science*. 2005;308(5725):1181–1184.
33. Hoogeboom D, Essers MA, Polderman PE, Voets E, Smits LM, Burgering BM. Interaction of FOXO with beta-catenin inhibits beta-catenin/T cell factor activity. *J Biol Chem*. 2008;283(14):9224–9230.
34. Almeida M, Han L, Martin-Millan M, O'Brien CA, Manolagas SC. Oxidative stress antagonizes Wnt signaling in osteoblast precursors by diverting beta-catenin from T cell factor- to forkhead box O-mediated transcription. *J Biol Chem*. 2007;282(37):27298–27305.
35. Thorne CA, et al. Small-molecule inhibition of Wnt signaling through activation of casein kinase 1α. *Nat Chem Biol*. 2010;6(11):829–836.
36. Qiao X, et al. Redirecting TGF-β signaling through the β-catenin/Foxo complex prevents kidney fibrosis. *J Am Soc Nephrol*. 2018;29(2):557–570.
37. Luo Q, et al. Connective tissue growth factor (CTGF) is regulated by Wnt and bone morphogenetic proteins signaling in osteoblast differentiation of mesenchymal stem cells. *J Biol Chem*. 2004;279(53):55958–55968.
38. He W, et al. Plasminogen activator inhibitor-1 is a transcriptional target of the canonical pathway of Wnt/beta-catenin signaling. *J Biol Chem*. 2010;285(32):24665–24675.
39. Lee HJ, et al. Hydrogen sulfide inhibits high glucose-induced NADPH oxidase 4 expression and matrix increase by recruiting inducible nitric oxide synthase in kidney proximal tubular epithelial cells. *J Biol Chem*. 2017;292(14):5665–5675.
40. Wu D, et al. Hydrogen sulfide ameliorates chronic renal failure in rats by inhibiting apoptosis and inflammation through ROS/MAPK and NF-κB signaling pathways. *Sci Rep*. 2017;7(1):455.
41. Han SJ, et al. Hydrogen sulfide-producing cystathionine γ-lyase is critical in the progression of kidney fibrosis. *Free Radic Biol Med*. 2017;112:423–432.
42. DiRocco DP, Kobayashi A, Taketo MM, McMahon AP, Humphreys BD. Wnt4/β-catenin signaling in medullary kidney myofibroblasts. *J Am Soc Nephrol*. 2013;24(9):1399–1412.
43. Zhou D, et al. Tubule-derived Wnts are required for fibroblast activation and kidney fibrosis. *J Am Soc Nephrol*. 2017;28(8):2322–2336.
44. Emami KH, et al. A small molecule inhibitor of beta-catenin/CREB-binding protein transcription [corrected]. *Proc Natl Acad Sci U S A*. 2004;101(34):12682–12687.
45. Huber AH, Nelson WJ, Weis WI. Three-dimensional structure of the armadillo repeat region of beta-catenin. *Cell*. 1997;90(5):871–882.
46. Schelling JR, Nkemere N, Kopp JB, Cleveland RP. Fas-dependent fratricidal apoptosis is a mechanism of tubular epithelial cell deletion in chronic renal failure. *Lab Invest*. 1998;78(7):813–824.
47. Khan S, Cleveland RP, Koch CJ, Schelling JR. Hypoxia induces renal tubular epithelial cell apoptosis in chronic renal disease. *Lab Invest*. 1999;79(9):1089–1099.
48. Schelling JR, Cleveland RP. Involvement of Fas-dependent apoptosis in renal tubular epithelial cell deletion in chronic renal failure. *Kidney Int*. 1999;56(4):1313–1316.
49. Schelling JR. Tubular atrophy in the pathogenesis of chronic kidney disease progression. *Pediatr Nephrol*. 2016;31(5):693–706.
50. Kumar D, Robertson S, Burns KD. Evidence of apoptosis in human diabetic kidney. *Mol Cell Biochem*. 2004;259(1-2):67–70.
51. Susztak K, Ciccone E, McCue P, Sharma K, Böttinger EP. Multiple metabolic hits converge on CD36 as novel mediator of tubular epithelial apoptosis in diabetic nephropathy. *PLoS Med*. 2005;2(2):e45.
52. Wong DWL, et al. Activated renal tubular Wnt/β-catenin signaling triggers renal inflammation during overload proteinuria. *Kidney Int*. 2018;93(6):1367–1383.
53. Kato H, et al. Wnt/β-catenin pathway in podocytes integrates cell adhesion, differentiation, and survival. *J Biol Chem*. 2011;286(29):26003–26015.
54. Liu H, et al. Wnt signaling regulates hepatic metabolism. *Sci Signal*. 2011;4(158):ra6.
55. Iyer S, et al. FOXOs attenuate bone formation by suppressing Wnt signaling. *J Clin Invest*. 2013;123(8):3409–3419.
56. Liu H, et al. FOXO3a modulates WNT/β-catenin signaling and suppresses epithelial-to-mesenchymal transition in prostate cancer cells. *Cell Signal*. 2015;27(3):510–518.
57. Rao P, et al. Promotion of β-catenin/Foxo1 signaling ameliorates renal interstitial fibrosis. *Lab Invest*. 2019;99(11):1689–1701.
58. Li Y, Meng R. MicroRNA-154 targets the Wnt/β-catenin signaling pathway following injury to human vascular endothelial cells by hydrogen peroxide. *Med Sci Monit*. 2019;25:5648–5656.
59. Huang S, Li H, Ge J. A cardioprotective insight of the cystathionine γ-lyase/hydrogen sulfide pathway. *Int J Cardiol Heart Vasc*. 2015;7:51–57.
60. Yamamoto J, et al. Distribution of hydrogen sulfide (H_2S)-producing enzymes and the roles of the H_2S donor sodium hydrosulfide in diabetic nephropathy. *Clin Exp Nephrol*. 2013;17(1):32–40.
61. Szabó C. Hydrogen sulphide and its therapeutic potential. *Nat Rev Drug Discov*. 2007;6(11):917–935.
62. Suzuki K, et al. Hydrogen sulfide replacement therapy protects the vascular endothelium in hyperglycemia by preserving mitochondrial function. *Proc Natl Acad Sci U S A*. 2011;108(33):13829–13834.
63. Whiteman M, et al. The novel neuromodulator hydrogen sulfide: an endogenous peroxynitrite 'scavenger'? *J Neurochem*. 2004;90(3):765–768.
64. Li L, Kang H, Zhang Q, D'Agati VD, Al-Awqati Q, Lin F. FoxO3 activation in hypoxic tubules prevents chronic kidney disease. *J Clin Invest*. 2019;129(6):2374–2389.

65. Zhou D, et al. Fibroblast-specific β-catenin signaling dictates the outcome of AKI. *J Am Soc Nephrol*. 2018;29(4):1257–1271.
66. Cohen CD, et al. Improved elucidation of biological processes linked to diabetic nephropathy by single probe-based microarray data analysis. *PLoS One*. 2008;3(8):e2937.
67. Fiorentino L, et al. Loss of TIMP3 underlies diabetic nephropathy via FoxO1/STAT1 interplay. *EMBO Mol Med*. 2013;5(3):441–455.
68. Maclean KN, et al. Cystathionine protects against endoplasmic reticulum stress-induced lipid accumulation, tissue injury, and apoptotic cell death. *J Biol Chem*. 2012;287(38):31994–32005.
69. Perna AF, et al. Hydrogen sulphide-generating pathways in haemodialysis patients: a study on relevant metabolites and transcriptional regulation of genes encoding for key enzymes. *Nephrol Dial Transplant*. 2009;24(12):3756–3763.
70. Skrypnyk NI, Harris RC, de Caestecker MP. Ischemia-reperfusion model of acute kidney injury and post injury fibrosis in mice. *J Vis Exp*. 2013;(78):50495.
71. Gewin L, et al. TGF-beta receptor deletion in the renal collecting system exacerbates fibrosis. *J Am Soc Nephrol*. 2010;21(8):1334–1343.
72. Cox B, Emili A. Tissue subcellular fractionation and protein extraction for use in mass-spectrometry-based proteomics. *Nat Protoc*. 2006;1(4):1872–1878.
73. Nlandu-Khodo S, et al. Blocking TGF-β and β-catenin epithelial crosstalk exacerbates CKD. *J Am Soc Nephrol*. 2017;28(12):3490–3503.
74. Sheng Q, et al. Multi-perspective quality control of Illumina RNA sequencing data analysis. *Brief Funct Genomics*. 2017;16(4):194–204.
75. Guo Y, et al. Multi-perspective quality control of Illumina exome sequencing data using QC3. *Genomics*. 2014;103(5-6):323–328.
76. Trapnell C, Pachter L, Salzberg SL. TopHat: discovering splice junctions with RNA-Seq. *Bioinformatics*. 2009;25(9):1105–1111.
77. Trapnell C, et al. Transcript assembly and quantification by RNA-Seq reveals unannotated transcripts and isoform switching during cell differentiation. *Nat Biotechnol*. 2010;28(5):511–515.